ACS Catalysis

Research Article

pubs.acs.org/acscatalysis

Efficient and Durable Au Alloyed Pd Single-Atom Catalyst for the Ullmann Reaction of Aryl Chlorides in Water

Leilei Zhang,[†,‡] Aiqin Wang,*[,†] Jeffrey T. Miller,[§] Xiaoyan Liu,[†] Xiaofeng Yang,[†] Wentao Wang,[†] Lin Li,[†] Yanqiang Huang,[†] Chung-Yuan Mou,[∥] and Tao Zhang*[,†]

[†]State Key Laboratory of Catalysis, Dalian Institute of Chemical Physics, Chinese Academy of Sciences, Dalian 116023, China

[‡]University of Chinese Academy of Sciences, Beijing 100049, China

[§]CSE, Argonne National Laboratory, 9700 S. Cass Avenue, Argonne, Illinois 60439, United States

[∥]Department of Chemistry, National Taiwan University, Taipei 10617, Taiwan

Supporting Information

ABSTRACT: Ion exchange resin supported Au alloyed Pd single atoms have been explored to serve as an effective and robust catalyst for the Ullmann reaction of aryl halides under mild conditions in aqueous media, in particular for the activation of less reactive aryl chlorides. The catalysts were prepared with an ion exchange-$NaBH_4$ reduction method and submitted to extensive characterizations by HRTEM, XRD, EXAFS, and DRIFTS techniques. XRD patterns demonstrated the formation of Au−Pd alloys. EXAFS and DRIFTS characterization results showed that with an increase of Au/Pd molar ratios, the continuous Pd ensembles on the surface were gradually separated and eventually isolated by Au atoms, confirming that the Au alloyed Pd single-atom catalyst was formed. The catalysts exhibited excellent performance for the Ullmann reaction of aryl chlorides, and the turnover number (TON) increased exponentially with a decrease of the amount of Pd in the catalysts. On the basis of these characterization and catalytic results, the Au alloyed Pd single-atom was proposed as the active site for the reaction. The catalyst exhibited excellent catalytic performance for a broad scope of substrates and could be reused at least 8 times with no change in yield. This Au alloyed Pd single-atom catalyst bridges the gap between homogeneous and heterogeneous catalysis in organic transformations and may open a new vision to develop other efficient single-atom catalysts for green synthesis of fine chemicals.

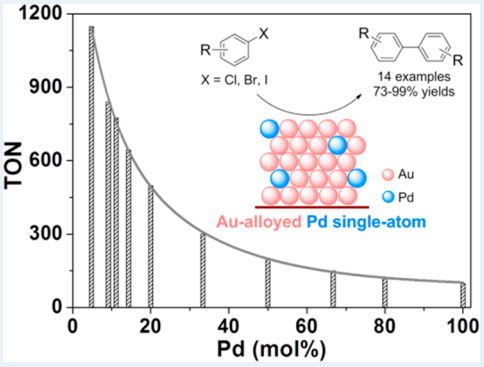

KEYWORDS: *Ullmann reaction, aryl chlorides, heterogeneous catalyst, Au−Pd alloy, Pd single-atom*

1. INTRODUCTION

The Pd catalyzed Ullmann reaction is a versatile methodology for the synthesis of complex organic molecules such as pharmaceuticals, medicine, polymers, alkaloids, and other advanced materials.[1,2] Great progress has been made in homogeneous Pd catalysts.[3−7] The specifically designed molecular Pd metal−ligand complex, usually made up of a Pd monomer and N, O, S, and P donor ligands, could provide high activity and selectivity in the Ullmann reaction of aryl halides due to the geometric and electronic contributions of these ligands to central Pd active site.[8] The difficulties in recovery and reuse of the homogeneous Pd catalysts, however, compromised their high efficiency and limited their applications. Therefore, enormous interest and effort in recent years have been devoted to heterogeneous Pd catalysts to overcome the shortcomings of homogeneous Pd catalysts.[9−13] Supported Pd nanoparticles could be easily recycled but, in turn, suffered from the inefficient utilization of the expensive Pd metal. Furthermore, protocols of Pd nanoparticles that work well with aryl chlorides are rare because of the chemical inertness of aryl chlorides relative to aryl bromides and iodides.[14,15] Nevertheless, the use of aryl chlorides as the substrates is highly desirable for they are more readily available, cheaper, and even more environmentally strategic than the analogues of bromides and iodides.[16−18] Therefore, it would be highly desirable while rather challenging to design and develop new types of supported Pd catalysts that are able to catalyze the Ullmann reaction of aryl chlorides with high efficiency and durability.

In view of the key role of ligands in homogeneous Pd catalysts, we envisage that by employing a second metal, or a suitable support to mimic the steric and/or electronic environment of ligands surrounding the Pd atoms, a highly active and durable heterogeneous catalyst would be produced. Recently, we developed a new type of heterogeneous catalyst, a single-atom catalyst, which contains exclusively single atoms either stabilized by the support underneath or isolated by another metal atom.[19−21] The single-atom catalyst is expected to bridge the gap between homogeneous and heterogeneous

Received: January 18, 2014
Revised: April 2, 2014
Published: April 3, 2014

   dx.doi.org/10.1021/cs500071c | ACS Catal. 2014, 4, 1546−1553

catalysts.[22] Nevertheless, so far there has not been any practical example to demonstrate this expectation in organic transformations.

Alloying Pd with IB group metal has proved a promising method for constructing Pd single-atom catalysts wherein Pd active sites are isolated by Au, Ag, or Cu atoms.[23−27] In particular, Au-alloyed Pd single-atom catalysts will have great potentials in organic transformations by combining the merits of homogeneous and heterogeneous catalysts. On account of the good miscibility and the unique interplay between Au and Pd atoms, the neighboring coordinated Au atoms not only stabilize the central Pd atom but also modify the electronic properties of Pd.[19] Furthermore, Pd atoms located at distinct positions, such as corner, edge, and terrace sites, are supposed to have different coordination environments and electronic structure.[28,29] In this regard, Au alloyed Pd single-atom catalysts can be considered as structural mimics of the homogeneous counterpart but with heterogeneous merit and better stability, and unique catalytic performances could be expected.

Herein we for the first time report that ion-exchange resin supported Au alloyed Pd single atoms serve as an effective and robust catalyst for the Ullmann reaction of aryl chlorides in aqueous media. The catalyst exhibited high activity and excellent stability with broad substrate scope and functional group tolerance. The high atom efficiency, combined with the unique geometrical structure and the electronic properties of the special active site entities, made the Au alloyed Pd single atoms a unique catalyst for aryl chloride activation.

2. EXPERIMENTAL SECTION

2.1. Catalyst Preparation. $HAuCl_4{\cdot}3H_2O$ and $PdCl_2$ were purchased from Shanghai Chemical Reagent Co., Ltd., and 717# ion-exchange resin was provided by Sinopharm Chemical Reagent Co., Ltd. Other chemicals were purchased from Tianjin Kemiou Chemical Reagent Co., Ltd. All chemicals were of analytical grade and used as received without further purification. The water used in this study was deionized by a Milli-Q Plus system, having 18.2 MΩ electrical resistivity.

An aqueous solution of $HAuCl_4$ with a concentration of 9.56 mg_{Au}/mL was prepared by dissolving 1.0 g of $HAuCl_4{\cdot}3H_2O$ in 50.0 mL of Milli-Q water. An aqueous solution of H_2PdCl_4 with a concentration of 12.00 mg_{Pd}/mL was prepared by dissolving 1.0 g of $PdCl_2$ in 1.5 mL of 12 mol/L HCl, and then diluted to 50.0 mL with Milli-Q water.

717# anion exchange resin was washed by water several times until the filtrate became clean. After drying at 60 °C, the resin was crushed with a ball mill at 250 rpm for 1 h and then sieved to 100−180 mesh for use as the catalyst support. The resin support was then soaked sequentially in 1.0 mol/L NaOH, 1.0 mol/L HNO_3, and 1.0 mol/L NaOH for 8 h, and finally in 2.0 mol/L K_2CO_3 solution for 24 h. The resultant ion-exchange resin was filtered and washed with water until the filtrate became neutral and then dried under vacuum at 60 °C for 12 h.

The ion-exchange resin supported Au alloyed Pd single-atom catalyst was prepared with an anion exchange-$NaBH_4$ reduction method as described earlier.[30] Specifically, 1.92 mL of 9.56 mg_{Au}/mL $HAuCl_4$ solution and 0.14 mL of 12.00 mg_{Pd}/mL H_2PdCl_4 were added to 200 mL of water, followed by the addition of 1.0 g of support and stirring for 2 h under darkness. After recovery by thorough washing and filtration, the solid was redispersed in 30.0 mL of water, and followed by the addition of 15.0 mL of $NaBH_4$ (10.0 equiv) solution. The mixture turned immediately from orange to dark brown. After being stirred under darkness for another 0.5 h, the catalyst was filtered and washed thoroughly with water until no Cl^- was detected and then dried at 60 °C for 8 h under vacuum. The resultant catalyst was denoted as Au_6Pd/resin. For comparison, monometallic Au/resin, Pd/resin, and bimetallic Au−Pd/resin with various Au/Pd atomic ratios were also synthesized with the same method but variation of the volumes of precursor solutions. For all the catalysts with different Au/Pd molar ratios, the total metal loading was controlled at 2.0 wt %.

2.2. Catalyst Characterizations. In situ X-ray powder diffraction (XRD) analysis was carried out on a PANalytical X'pert diffractometer using nickel-filtered Cu Kα radiation with a scanning angle (2θ) of 10°−80°, operated at 40 kV and 40 mA. Before the XRD patterns were collected, the samples were in situ reduced in pure H_2 at 80 °C for 30 min.

The metal loadings of the catalysts were determined with inductively coupled plasma atomic emission spectroscopy (ICP-AES) on an IRIS Intrepid II XSP instrument (Thermo Electron Corp.). Before examination, a proper amount of powdered sample was treated by hot aqua regia (*Caution: Hot aqua regia is highly corrosive*).

High resolution transmission electron microscope (HRTEM) characterization was carried out with a Tecnai G^2 Spirit (FEI) microscope operating at 200 kV. Prior to observations, the powdered sample of the catalyst was ultrasonically dispersed in ethanol, and a few droplets of the suspension were put on copper grids covered with a holey carbon film and dried at room temperature.

The diffuse reflectance infrared Fourier transform spectroscopy (DRIFTS) characterization was performed with a Bruker Equinox 55 spectrometer equipped with a MCT detector and operated at a resolution of 4 cm^{-1}. The sample was in situ reduced in pure H_2 at 80 °C for 30 min and purged with pure He at 90 °C for 10 min, then cooled to room temperature to collect the background spectra. Subsequently, the sample was exposed to a flowing mixture of 5.0 vol % CO in He to collect the spectra at a given time interval until the intensity was no longer increased, followed by purging with pure He to remove the gas phase CO. For DRIFT spectra with an increase of CO pressure, the reduced sample was evacuated at 90 °C and then cooled to room temperature to collect the background spectra. Subsequently, a dose of CO at a very low pressure was admitted to the cell, followed by evacuating the cell to the desired vacuum before the spectra were collected.

X-ray absorption fine structure (XAFS) spectra at Au L_{III}-edge and Pd K-edge were recorded at three beamlines. Two samples ($Au_{10}Pd$ and Au_6Pd) were measured at the 01C1 beamline of National Synchrotron Radiation Research Center, Hsinchu, Taiwan. Four samples (Au, Au_4Pd, $AuPd_2$, and Pd) were measured on the insertion-device beamline 10-ID-B of the Materials Research Collaborative Access Team (MRCAT) at the Advanced Photon Source at Argonne National Laboratory. One sample (AuPd) was measured at 14W beamline of Shanghai Synchrotron Radiation Facility (SSRF). The three beamlines employed a double Si (111)-crystal monochromator for energy selection with a resolution better than 2×10^{-4} at both the Au L_{III}-edge and Pd K-edge. The powdery catalyst was packed into the middle part of a quartz glass tube, both ends of which were sealed with Kapton film. Before measurement, the sample was reduced in pure H_2 at 80 °C followed by purging with pure N_2. The X-ray absorption spectra at Au L_{III}-edge and Pd K-edge were recorded at room temperature in transmission and fluorescence mode, respectively. Au foil or Pd foil as

dx.doi.org/10.1021/cs500071c | ACS Catal. 2014, 4, 1546−1553

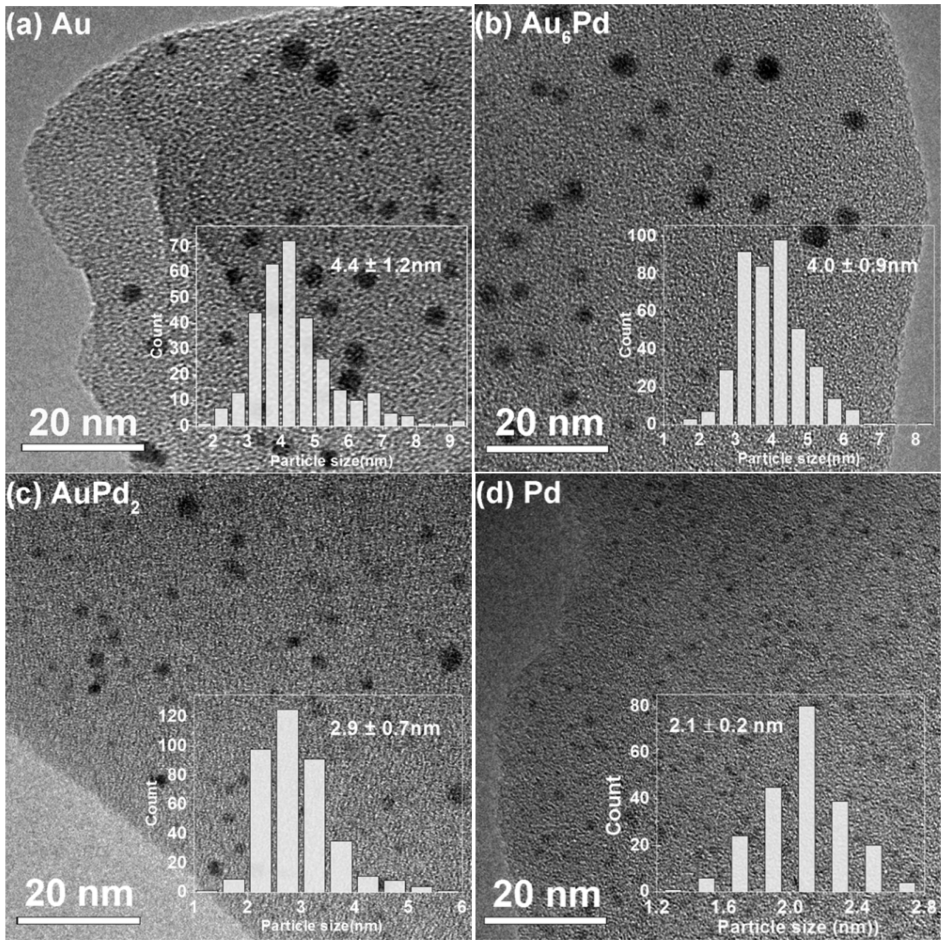

Figure 1. HRTEM images of (a) Au/resin, (b) Au_6Pd/resin, (c) $AuPd_2$/resin, and (d) Pd/resin.

standard compound was measured simultaneously by using the third ionization chamber so that energy calibration could be performed scan by scan. The X-ray absorption data were processed by the Athena software package.

Gas chromatography (GC) analysis was performed on an Agilent 6890N system equipped with a 5% phenyl methyl siloxane capillary column (30 m × 320 μm × 0.25 μm). The GC yield was obtained from the calibration curve using 1,3,5-trimethylbenzene as an internal standard.

^{1}H NMR spectra were recorded on commercial instruments (500 MHz). Chemical shifts were reported in ppm from tetramethylsilane with the solvent resonance as the internal standard ($CDCl_3$, δ = 7.26). ^{13}C NMR spectra were collected on commercial instruments (125 MHz) with complete proton decoupling. Chemical shifts are reported in ppm from the tetramethylsilane with the solvent resonance as internal standard ($CDCl_3$, δ = 77.0). The structures of the known compounds were confirmed by comparison with commercially available compounds or data shown in literature.

2.3. Catalyst Evaluation. Unless otherwise noted, the Ullmann reactions were carried out as follows: a mixture of Ar-X (1.00 mmol), ascorbic acid (176 mg, 1.0 equiv), sodium hydroxide (3.0 mmol in 2.5 mL H_2O, 3.0 equiv), and Au_6Pd/resin (93 mg, 1.0 mol %) were put in the reactor and vigorously stirred at 80 °C for 3 h. After cooling down to room temperature, the catalyst was separated by filtration and washed with ethyl acetate (15.0 mL). After adding 10.0 mL of H_2O, the filtrate was extracted with ethyl acetate (3 × 15.0 mL). The combined organic layer was washed by saturated NaCl solution and dried over anhydrous magnesium sulfate. After filtration to remove magnesium sulfate, volatile substances were removed under reduced pressure to yield the final biphenyl.

The amount of Au−Pd/resin catalyst employed in the reaction was calculated based on the total moles of the two metals (Au + Pd). Take Au_6Pd/resin, for example, for 1.0 g Au_6Pd/resin catalyst, the total moles of the two metals were calculated as follows: 1 g × 1.82 wt %/197.0 g/mol + 1 g × 0.16 wt %/106.4 g/mol = 0.107 mmol. For the 1.0 mmol substrate, the weight of Au_6Pd/resin was 1.0 mmol × 1 mol %/0.107 mmol/g = 0.093 g.

3. RESULTS AND DISCUSSION

3.1. HRTEM and XRD Characterization. HRTEM images and size distribution histograms of four representative samples are shown in Figure 1. The nanoparticles with a mean size of 2−4 nm are highly dispersed on the support. Moreover, with an increase of the Pd content, the average particle sizes of the samples present a decreasing trend, which is attributable to the higher melting point and thereby to the better antisintering property of Pd than that of Au. Consistent with the HRTEM result, the XRD patterns of the series of Au−Pd/resin catalysts shown in Figure 2 indicate clearly that the (111) reflection at 2θ = 38−40° becomes broader with an increase of the Pd fraction. More important, it is found that the (111) reflection position has a continual shift toward lower 2θ degrees with a decrease of the Pd content (see the inset), indicating the

dx.doi.org/10.1021/cs500071c | ACS Catal. 2014, 4, 1546−1553

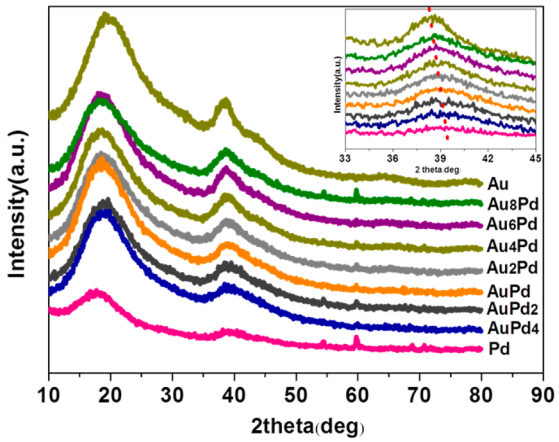

Figure 2. XRD patterns of Au/resin, Pd/resin, and Au–Pd/resin with different Au/Pd ratios. The inset is the enlargement of the profiles between 2θ = 33–45° showing a gradual shift of the peak toward a lower degree with an increase of the Au/Pd ratio.

formation of an Au–Pd alloy rather than core–shell structure.[31−33]

3.2. EXAFS Analysis. The electronic and structural information on the catalysts is obtained from XAFS (X-ray absorption fine structure) characterization.[34] The measurement was performed at the Au L_{III}-Edge and Pd K-edge, and the analysis results of the EXAFS (extended X-ray absorption fine structure) data are summarized in Table 1. It is noted that the

Table 1. Analysis Results of the EXAFS Data at the Pd K-Edge and Au L_{III}-Edge[a]

samples	scatter	N	$\sigma^2 \times 10^2$	ΔE_0 (eV)	R (Å)
Au	Au–Au	7.1	2.0	−1.0	2.80
$Au_{10}Pd$	Pd–Au	9.2	1.19	−7.4	2.79
	Au–Au	8.0	1.05	3.1	2.80
	Au–Pd	1.0	1.44	3.1	2.79
Au_6Pd	Pd–Pd	1.0	1.11	−7.3	2.82
	Pd–Au	7.7	1.11	−7.3	2.79
	Au–Au	7.6	1.01	3.0	2.80
	Au–Pd	1.2	1.19	4.5	2.79
Au_4Pd	Pd–Pd	1.8	2.0	−4.9	2.78
	Pd–Au	6.9	2.0	−3.8	2.80
	Au–Au	6.8	1.5	−0.6	2.82
	Au–Pd	1.5	1.5	5.0	2.76
$AuPd_2$	Pd–Pd	5.0	3.0	1.5	2.80
	Pd–Au	2.7	2.0	−9.3	2.78
	Au–Au	5.4	1.5	0.1	2.84
	Au–Pd	4.2	1.5	5.0	2.78
Pd	Pd–Pd	7.3	3.0	−0.1	2.77

[a] N is the coordination number for the absorber–backscatterer pair, R is the average absorber–backscatterer distance, σ^2 is the Debye–Waller factor, and ΔE_0 is the inner potential correction.

total coordination numbers (CN = 7–9) of all of the investigated samples are significantly smaller than those in bulk materials (CN = 12), in agreement with the very small particle sizes visualized by HRTEM. For Au–Pd/resin bimetallic catalysts, there are remarkable contributions from heteroatom bonding (Au–Pd and Pd–Au) in addition to Au–Au and Pd–Pd contributions, indicating the formation of an alloy phase. Moreover, with an increase of the Au/Pd ratio, the coordination number of Pd–Au increased while that of Pd–Pd decreased. In particular, when the Au/Pd ratio was ≥4, the contribution from Pd–Pd coordination was reduced remarkably and became negligible, indicating that most of the Pd atoms are isolated by gold. At an Au/Pd ratio ≥10, the Pd–Pd coordination disappeared completely, implying that the configuration of the Pd singleton surrounded by Au atoms, i.e., the Au alloyed Pd single-atom, is formed. The similar structure was also reported with other supported Au–Pd or Ag–Pd catalysts.[19,24]

3.3. DRIFTS Study. Since EXAFS provides only average structural information on a given material while catalysis is more relevant to surface structure, we further probed the surface structure and composition with CO-adsorbed FT-IR technique. CO adsorption on Pd prefers the bridging or hollow sites much more than atop sites, whereby the geometric structures of Au–Pd bimetallic surfaces can be effectively probed.[35−39] Figure 3 displays the DRIFT (diffuse reflection

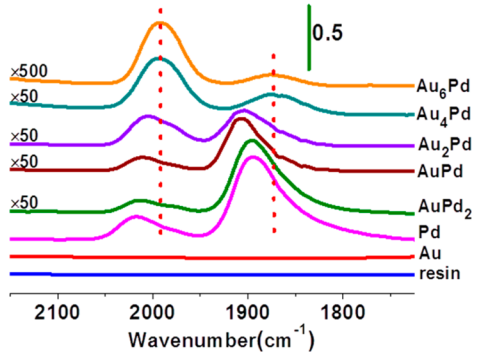

Figure 3. DRIFT spectra of CO adsorption on Au–Pd/resin catalysts with different Au/Pd atomic ratios.

infrared Fourier transform) spectra of CO adsorption on the samples with various Au/Pd atomic ratios. For a monometallic Au/resin catalyst, no band due to CO adsorption was observed, which is quite different from a oxide-supported gold nanocatalyst.[40,41] This result suggests that the resin support may weaken the adsorption of CO on gold. However, for the monometallic Pd/resin catalyst, two absorption bands centered at 1895 and 2020 cm^{-1} were clearly discerned. The former was much stronger than the latter and could be assigned to CO adsorbed on 2-fold bridging or 3-fold hollow sites, while the latter was broad with a shoulder and could be assigned to CO adsorbed on atop sites of Pd.[35−37] Compared with oxide-supported Pd nanocatalysts,[38] the CO band on atop sites of Pd/resin had a remarkable shift toward low frequency, again suggesting the resin support may impose an electronic effect on the Pd nanoparticles thereon. The presence of the shoulder associated with the band 2020 cm^{-1} implies that there are two types of atop sites on Pd nanoparticles.[38] For Au–Pd/resin bimetallic catalysts, the intensity of the CO adsorption bands was attenuated by more than 50-fold due to the dilution effect of Au. Moreover, with an increase of Au/Pd ratio, the intensity of bridged CO decreased gradually until it almost disappeared at Au/Pd ≥ 4, while that of atop CO increasingly dominated. This trend indicates that continuous surface Pd ensembles are separated gradually by Au atoms, leaving mostly isolated Pd atoms when Au/Pd ≥ 4. Further investigations of the DRIFT spectra with increasing CO pressure corroborated this trend: the frequency of atop CO did not change while that of bridged CO blue-shifted with increasing CO pressure due to the

dx.doi.org/10.1021/cs500071c | ACS Catal. 2014, 4, 1546−1553

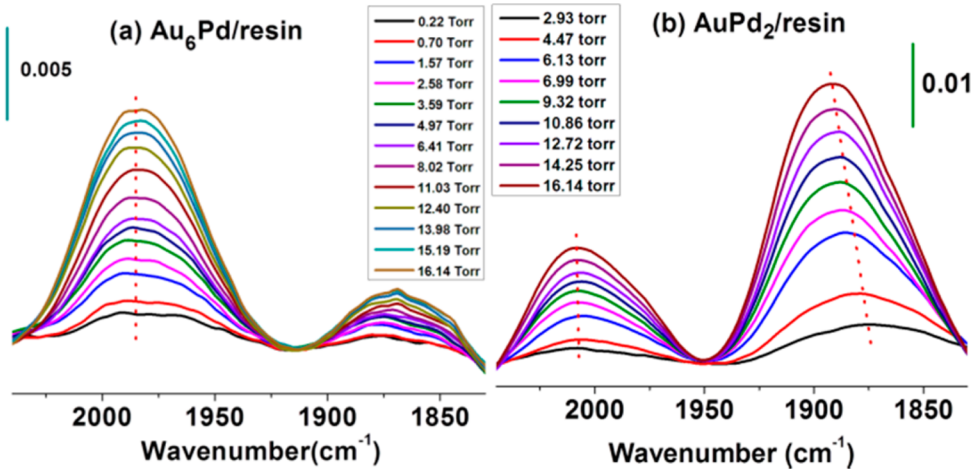

Figure 4. FTIR spectra of CO adsorption at different CO pressure on Au_6Pd/resin (a) and $AuPd_2$/resin (b).

dipole−dipole coupling effect (Figure 4).[20,39] Obviously, the DRIFTS result is in good agreement with the EXAFS result, providing compelling evidence that the Au alloyed Pd single-atom configuration is formed at Au/Pd ≥ 4. Another interesting phenomenon in the DRIFT spectra is that there is an irregular shift in bridged CO with Au/Pd ratio, which may be a collective effect from electronic modification, size variation, and ensemble effect.[39,42]

3.4. Catalytic Performance. The catalytic performance of the Au alloyed Pd single-atom catalyst was subsequently evaluated in the Ullmann coupling reaction. As aryl chlorides are much more difficult to activate than aryl bromides and iodides, coupling of chlorobenzene was first tested. The reaction was carried out in aqueous media in consideration of the environmentally benign process. Optimization of the reaction conditions showed that ascorbic acid (Vc) was the most effective reductant while NaOH was the suitable base (Tables S1−S2, Supporting Information). Under optimized reaction conditions, the activities of Au−Pd/resin with various Au/Pd ratios as well as their monometallic counterparts are summarized in Table 2. It can be seen that monometallic Pd/resin was effective for the Ullmann coupling reaction of chlorobenzene, affording a biphenyl yield of 81.9% (Table 2, entry 11), whereas monometallic Au/resin was totally inactive for this reaction (Table 2, entry 1). For the series of Au−Pd/resin bimetallic catalyst, the biphenyl yield increased first with the Au/Pd ratio and reached a maximum of 96.7% at an Au/Pd ratio of 2/1 (Table 2, entry 7), and then decreased with a further increase of the Au/Pd ratio, demonstrating a strong synergistic effect between Au and Pd. The selectivity was also enhanced first with Au/Pd ratio. For example, Pd/resin gave a biphenyl selectivity of 84.1% (Table 2, entry 11), while Au_6Pd/resin gave 99% (Table 2, entry 5). However, at a higher Au/Pd ratio (Au/Pd > 6), the selectivity decreased due to the dehalogenation reaction of chlorobenzene. In order to better demonstrate the synergistic effect between Pd and Au, we also compared the catalytic performances of 0.5 wt % Pd/resin and 2% Au_2Pd/resin; both of them have the same Pd concentration. From entry 12 and entry 7 in Table 2, one can see that the biphenyl yield over the 0.5 wt % Pd/resin was only 6.0%, which was much lower than that on 2% Au_2Pd/resin (96.7%).

Since Pd served as the main active component, we calculated the turnover number (TON) of different catalysts normalized by the total Pd mass, which gave an interesting trend. As illustrated in Figure 5, the TON increased almost exponentially with Au/Pd ratios; especially at Au/Pd ≥ 4/1 (corresponding to a molar concentration of Pd ≥ 20%), the enhancement rate was accelerated. From both EXAFS and DRIFTS character-

Table 2. Ullmann Coupling of Chlorobenzene over Au−Pd/Resin Catalysts with Various Au/Pd Ratios

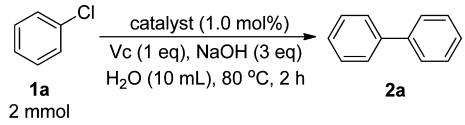

entry	catalyst	yield (%)[a]	selectivity (%)
1	Au/resin	0	
2	$Au_{20}Pd$/resin	42.2	73.4
3	$Au_{10}Pd$/resin	66.2	86.7
4	Au_8Pd/resin	81.7	94.9
5	Au_6Pd/resin	92.3	>99
6	Au_4Pd/resin	94.5	95
7	Au_2Pd/resin	96.7	96.7
8	AuPd/resin	91.4	91.4
9	$AuPd_2$/resin	89.0	89.3
10	$AuPd_4$/resin	84.6	84.8
11	Pd/resin	81.9	84.1
12[b]	Pd/resin	6.0	22.8

[a]Yield determined by GC using 1,3,5-trimethylbenzene as an internal standard. [b]The loading of Pd was 0.5 wt % in Pd/resin.

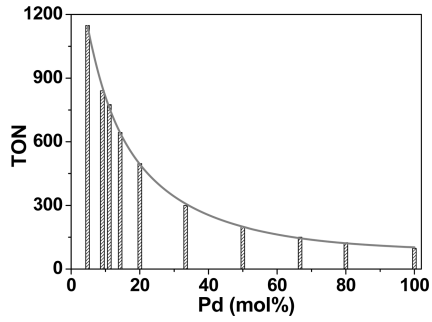

Figure 5. TON values of Au/resin, Pd/resin, and a series of Au−Pd/resin for the Ullmann reaction of chlorobenzene. The gray line is the exponentially fitted curve of TON as a function of Pd atomic percentage in the catalysts.

dx.doi.org/10.1021/cs500071c | ACS Catal. 2014, 4, 1546−1553

izations, we know that Au alloyed Pd single atoms dominate the surface structure at Au/Pd ratio ≥4/1. In other words, the more efficiently isolated by gold atoms, the more active are the resulting Pd single atoms. Therefore, correlating the activity with structure, we propose that the isolated Pd single atoms surrounded by Au atoms function as the active sites for the Ullmann coupling reaction of chlorobenzene. Such Au alloyed Pd single atoms are exceptionally active. For instance, Au_6Pd/resin affords a TON value of 643, which is 6.6-fold higher than that of Pd/resin; while $Au_{20}Pd$/resin gives a TON value of 1148 that is 1 order of magnitude higher than that of Pd/resin.

The exponential correlation curve of TON with the Pd fraction in the bimetallic catalyst is reminiscent of low-coordinated surface atoms as a function of particle size.[28,29,43] For pure the Pd/resin catalyst having an average Pd particle size of 2.1 nm, the fraction of surface atoms is estimated to be 48% assuming a cubic geometry, for which the low-coordinated atoms (corner and edge atoms) roughly account for 18%.[38] If the low-coordinated atoms are considered as the active sites for the Ullmann coupling reaction of chlorobenzene, the TON of Pd/resin is recalculated to be 1122, which is very close to that of $Au_{20}Pd$/resin. According to this calculation result, we can reasonably deduce that the low-coordinated corner and edge Pd atoms function as the main active sites, and the Pd single atoms isolated and surrounded by Au atoms in the Au−Pd nanoparticles should be mainly positioned at top (corner) sites. A reverse structure with Pd nanoparticles decorated by top gold atoms was recently reported by Toshima and co-workers, and the top gold atoms were found to be highly active for glucose oxidation.[28] These results suggest that the single-atom configuration formed by alloying two different metals will be an effective strategy to creating highly active single-site catalysts.

To demonstrate the general applicability of the Au alloyed Pd single-atom catalyst for the Ullmann reaction, the scope of substrates was investigated. As shown in Table 3, various aryl chlorides with different functional groups were converted successfully to the desired products with good to excellent yields. Specifically, for inactive aryl chlorides bearing electron-donating groups (Table 3, entries 2−6), the reaction proceeded very well, and the desired products could be obtained in high yields. Aryl chlorides containing electron-withdrawing groups also successfully underwent Ullmann coupling to afford the desired products (Table 3, entries 7−9). The Au alloyed Pd single-atom catalyst was also tolerant to aryl bromides and iodides (Table 3, entries 10−14), and the reaction could proceed smoothly under even milder reaction conditions to afford the desired products. This result is quite different from the work of Dhital et al. in which Au−Pd (1/1) alloy nanoclusters stabilized by PVP could efficiently catalyze the Ullmann coupling of chloroarenes but were rather poor for bromoarenes.[18] In a subsequent work, they reported that they found that aryl iodide was an even stronger inhibitor by forming a stable complex with a gold component.[44] In contrast, for our Au alloyed Pd single-atom catalyst, no such poisoning effect was observed. Instead, the Ullmann coupling reaction still follows the normal rule in regard to th ereactivity of the substrates: aryl chlorides ≪ aryl bromides < aryl iodides. Evidently, our Au alloyed Pd single-atom catalysts are more robust and adaptable to various substrates.

To verify whether the catalytic mechanism follows a heterogeneous or homogeneous catalysis path, hot filtration tests and kinetic studies were carried out.[45] The catalyst was

Table 3. Ullmann Reactions of Aryl Halides over Au_6Pd/Resin[a]

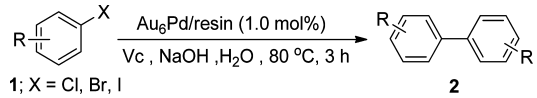

1; X = Cl, Br, I 2

Entry	Substrate	Product	2	T (°C)	t (h)	Yield (%)
1	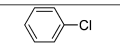	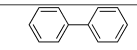	**2a**	80	3	89
2	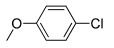	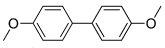	**2b**	80	6	97
3	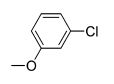	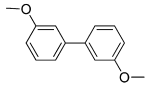	**2c**	80	6	98
4	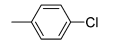	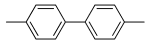	**2d**	80	6	84
5	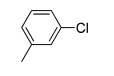	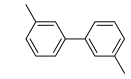	**2e**	80	6	80
6	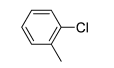	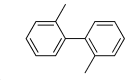	**2f**	80	6	73
7	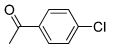	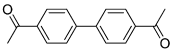	**2g**	80	3	99
8	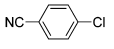	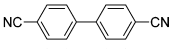	**2h**	80	3	77
9	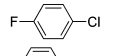	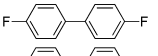	**2i**	80	3	88
10	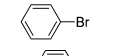	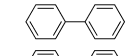	**2a**	60	3	99
11	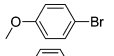	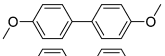	**2b**	80	3	93
12	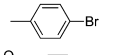	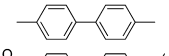	**2d**	80	3	91
13	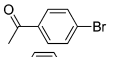		**2g**	60	3	90
14	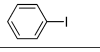	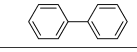	**2a**	60	1.5	99

[a]Reaction conditions: Au_6Pd/resin (1.0 mol %), **1** (1.0 mmol), Vc (1.0 mmol), NaOH (3.0 mmol), and H_2O (2.5 mL); isolated yield.

separated from the reaction mixture at a chlorobenzene conversion of 50.4% by hot filtration. ICP-AES examination of the filtrate showed that only 0.07 ppm (corresponding to 0.08 wt % of the initial charge) palladium was leached into the solution and that the reaction did not proceed when a new batch of substrate was added to the filtrate. Kinetic studies (Figure 6) showed that the reaction rate had no correlation

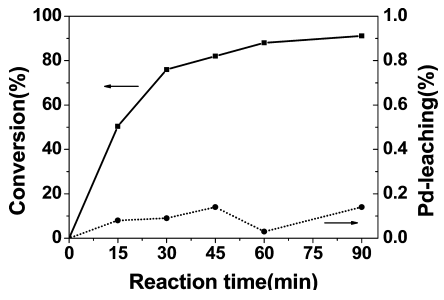

Figure 6. Kinetic studies of Ullmann reactions over Au_4Pd/resin.

with the content of leached Pd species in solution. Taken together, these results ruled out the possible contribution to the observed catalysis from Pd species leached into the reaction solution, and we ascertained that the reaction was intrinsically catalyzed by a heterogeneous catalyst.

dx.doi.org/10.1021/cs500071c | ACS Catal. 2014, 4, 1546−1553

One of the most important concerns about catalysts employed in liquid phase reactions is the durability. Therefore, we addressed the issue of recovery and reuse of the catalyst. The catalyst could be simply separated from the reaction mixture by filtration and reused in another batch of reaction after drying under vacuum. Figure 7 showed the catalyst could

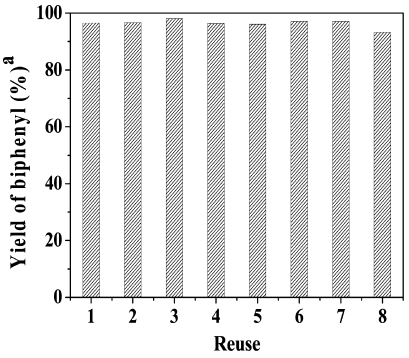

Figure 7. Recovery and reuse of Au_4Pd/resin for the Ullmann reaction. [a]: yield determined by GC using 1,3,5-trimethylbenzene as an internal standard.

be recycled for up to 8 times with no change in yield, demonstrating excellent reusability of the Au alloyed Pd single atom catalysts. In comparison with the quasi-homogeneous Au–Pd alloy nanoclusters reported by Dhital et al. that was difficult to recover and reuse,[18,44] our current single-atom catalyst system is obviously more suitable for practical applications because of its high activity, broad substrate scope, and excellent reusability.

4. CONCLUSIONS

In summary, using ion-exchange resin as the support, the Au alloyed Pd single-atom catalyst was prepared with a ion-exchange-$NaBH_4$ reduction method. EXAFS and DRIFTS characterization results showed that the surface Pd sites were totally isolated by Au atoms when Au/Pd $\geq$ 10, demonstrating the formation of the Pd single-atom configuration. The catalyst exhibited exceptional activity and excellent durability for Ullmann reactions of aryl chlorides as well as aryl bromides and iodides with broad substrate scope and could be reused 8 times with no change in yield. The uniform configuration of the Au alloyed Pd single-atom catalyst will make it function as a bridge between homogeneous and heterogeneous catalysts and may provide a new avenue to design and synthesize other efficient single-atom catalysts. Further investigation of the Au alloyed Pd single-atom catalysts for other liquid phase organic synthesis is underway.

■ ASSOCIATED CONTENT

Supporting Information

^1H NMR and ^{13}C NMR spectra and optimization of Ullmann reaction conditions. This material is available free of charge via the Internet at http://pubs.acs.org.

■ AUTHOR INFORMATION

Corresponding Authors

*(A.W.) E-mail: aqwang@dicp.ac.cn.

*(T.Z.) E-mail: taozhang@dicp.ac.cn.

Notes

The authors declare no competing financial interest.

■ ACKNOWLEDGMENTS

We are grateful to the National Science Foundation of China (21176235, 21203182, 21202163, 21303194, 21373206, and 21173218) and Hundred Talents Program of Dalian Institute of Chemical Physics (DICP). J.T.M. was funded by the U.S. Department of Energy, Office of Basic Energy Sciences, Chemical Sciences under Contract DE-AC-02-06CH11357. Use of the Advanced Photon Source is supported by the U.S. Department of Energy, Office of Science, and Office of Basic Energy Sciences, under Contract DE-AC02-06CH11357. MRCAT operations are supported by the Department of Energy and the MRCAT member institutions. We also thank Dr. Jyh-Fu Lee and Dr. Ting shan Chan from BL 17C1 and 01C1 at the National Synchrotron Radiation Research Center, Hsinchu, Taiwan, and the BL 14W at the Shanghai Synchrotron Radiation Facility (SSRF) for the EXAFS experiments.

■ REFERENCES

(1) Bringmann, G.; Walter, R.; Weirich, R. *Angew. Chem., Int. Ed.* **1990**, *29*, 977–991.
(2) Yin, L.; Liebscher, J. *Chem. Rev.* **2007**, *107*, 133–173.
(3) Herrmann, W. A.; Öfele, K.; Schneider, S. K.; Herdtweck, E.; Hoffmann, S. D. *Angew. Chem., Int. Ed.* **2006**, *45*, 3859–3862.
(4) Altenhoff, G.; Goddard, R.; Lehmann, C. W.; Glorius, F. *Angew. Chem., Int. Ed.* **2003**, *42*, 3690–3693.
(5) Snelders, D. J. M.; Koten, G. v.; Gebbink, R. J. M. K. *J. Am. Chem. Soc.* **2009**, *131*, 11407–11416.
(6) Pratap, R.; Parrish, D.; Gunda, P.; Venkataraman, D.; Lakshman, M. K. *J. Am. Chem. Soc.* **2009**, *131*, 12240–12249.
(7) Martin, R.; Buchwald, S. L. *Acc. Chem. Res.* **2008**, *41*, 1461–1473.
(8) Phan, N. T. S.; Sluys, M. V. D.; Jones, C. W. *Adv. Synth. Catal.* **2006**, *348*, 609–679.
(9) Yuan, B.; Pan, Y.; Li, Y.; Yin, B.; Jiang, H. *Angew. Chem., Int. Ed.* **2010**, *49*, 4054–4058.
(10) Wan, Y.; Wang, H.; Zhao, Q.; Klingstedt, M.; Terasaki, O.; Zhao, D. *J. Am. Chem. Soc.* **2009**, *131*, 4541–4550.
(11) Cho, J. K.; Najman, R.; Dean, T. W.; Ichihara, O.; Muller, C.; Bradley, M. *J. Am. Chem. Soc.* **2006**, *128*, 6276–6277.
(12) Scheuermann, G. M.; Rumi, L.; Steurer, P.; Bannwarth, W.; Mülhaupt, R. *J. Am. Chem. Soc.* **2009**, *131*, 8262–8270.
(13) Zhang, F.; Yin, J. W.; Chai, W.; Li, H. X. *ChemSusChem* **2010**, *3*, 724–727.
(14) Gallon, B. J.; Kojima, R. W.; Kaner, R. B.; Diaconescu, P. L. *Angew. Chem., Int. Ed.* **2007**, *46*, 7251–7254.
(15) Han, J.; Liu, Y.; Guo, R. *J. Am. Chem. Soc.* **2009**, *131*, 2060–2061.
(16) LeBlond, C. R.; Andrews, A. T.; Sun, Y.; Sowa, J. R., Jr. *Org. Lett.* **2001**, *3*, 1555–1557.
(17) Littke, A. F.; Fu, G. C. *Angew. Chem., Int. Ed.* **2002**, *41*, 4176–4211.
(18) Dhital, R. N.; Kamonsatikul, C.; Somsook, E.; Bobuatong, K.; Ehara, M.; Karanjit, S.; Sakurai, H. *J. Am. Chem. Soc.* **2012**, *134*, 20250–20253.
(19) Wei, X.; Yang, X.-F.; Wang, A.-Q.; Li, L.; Liu, X.-Y.; Zhang, T.; Mou, C.-Y.; Li, J. *J. Phys. Chem. C* **2012**, *116*, 6222–6232.
(20) Qiao, B.-T.; Wang, A.-Q.; Yang, X.-F.; Allard, L. F.; Jiang, Z.; Cui, Y.-T.; Liu, J.-Y.; Li, J.; Zhang, T. *Nat. Chem.* **2011**, *3*, 634–641.
(21) Lin, J.; Wang, A.-Q.; Qiao, B.-T.; Liu, X.-Y.; Yang, X.-F.; Wang, X.; Liang, J.; Li, J.; Liu, J.; Zhang, T. *J. Am. Chem. Soc.* **2013**, *135*, 15314–15317.
(22) Yang, X.-F.; Wang, A.-Q.; Qiao, B.-T.; Li, J.; Liu, J.-Y.; Zhang, T. *Acc. Chem. Res.* **2013**, *46*, 1740–1748.
(23) Kyriakou, G.; Boucher, M. B.; Jewell, A. D.; Lewis, E. A.; Lawton, T. J.; Baber, A. E.; Tierney, H. L.; Flytzani-Stephanopoulos, M.; Sykes, E. C. H. *Science* **2012**, *335*, 1209–1212.
(24) Slanac, D. A.; Hardin, W. G.; Johnston, K. P.; Stevenson, K. J. *J. Am. Chem. Soc.* **2012**, *134*, 9812–9819.

(25) Jirkovský, J. S.; Panas, I.; Ahlberg, E.; Halasa, M.; Romani, S.; Schiffrin, D. J. *J. Am. Chem. Soc.* **2011**, *133*, 19432−19441.
(26) Chen, M.; Kumar, D.; Yi, C.-W.; Goodman, D. W. *Science* **2005**, *310*, 291−293.
(27) Wang, A.-Q.; Liu, X.-Y.; Mou, C.-Y.; Zhang, T. *J. Catal.* **2013**, *208*, 258−271.
(28) Zhang, H.; Watanabe, T.; Okumura, M.; Haruta, M.; Toshima, N. *Nat. Mater.* **2012**, *11*, 49−52.
(29) Williams, W. D.; Shekhar, M.; Lee, W.-S.; Kispersky, V.; Delgass, W. N.; Ribeiro, F. H.; Kim, S. M.; Stach, E. A.; Miller, J. T.; Allard, L. F. *J. Am. Chem. Soc.* **2010**, *132*, 14018−14020.
(30) Zhang, L.-L.; Wang, W.-T.; Wang, A.-Q.; Cui, Y.-T.; Yang, X.-F.; Huang, Y.-Q.; Liu, X.-Y.; Liu, W.-G.; Son, J.-Y.; Oji, H.; Zhang, T. *Green Chem.* **2013**, *15*, 2680−2684.
(31) Liu, X.-Y.; Wang, A.-Q.; Wang, X.-D.; Mou, C.-Y.; Zhang, T. *Chem. Commun.* **2008**, 3187−3189.
(32) Li, W.-J.; Wang, A.-Q.; Liu, X.-Y.; Zhang, T. *Appl. Catal., A* **2012**, *433*−*434*, 146−151.
(33) Liu, X.-Y.; Wang, A.-Q.; Li, L.; Zhang, T.; Mou, C.-Y.; Lee, J.-F. *J. Catal.* **2011**, *278*, 288−296.
(34) Frenkel, A. I. *Chem. Soc. Rev.* **2012**, *41*, 8163−8178.
(35) Wei, T.; Wang, J.; Goodman, D. W. *J. Phys. Chem. C* **2007**, *111*, 8781−8788.
(36) Abbott, H. L.; Aumer, A.; Lei, Y.; Asokan, C.; Meyer, R. J.; Sterrer, M.; Shaikhutdinov, S.; Freund, H.-J. *J. Phys. Chem. C* **2010**, *114*, 17099−17104.
(37) Yi, C.-W.; Luo, K.; Wei, T.; Goodman, D. W. *J. Phys. Chem. B* **2005**, *109*, 18535−18540.
(38) Lear, T.; Marshall, R.; Lopez-Sanchez, J. A.; Jackson, S. D.; Klapötke, T. M.; Bäumer, M.; Rupprechter, G.; Freund, H.-J.; Lennon, D. *J. Chem. Phys.* **2005**, *123*, 174706−174718.
(39) Bazin, P.; Saur, O.; Lavalley, J. C.; Daturi, M.; Blanchard, G. *Phys. Chem. Chem. Phys.* **2005**, *7*, 187−194.
(40) Kolli, N. E.; Delannoy, L.; Louis, C. *J. Catal.* **2013**, *297*, 79−92.
(41) Hugon, A.; Delannoy, L.; Krafft, J.-M.; Louis, C. *J. Phys. Chem. C* **2010**, *114*, 10823−10835.
(42) Tsunoyama, H.; Ichikuni, N.; Sakurai, H.; Tsukuda, T. *J. Am. Chem. Soc.* **2009**, *131*, 7086−7093.
(43) Shimizu, K.; Sato, R.; Satsuma, A. *Angew. Chem., Int. Ed.* **2009**, *48*, 3982−3986.
(44) Dhital, R. N.; Kamonsatikul, C.; Somsook, E.; Satod, Y.; Sakurai, H. *Chem. Commun.* **2013**, *49*, 2542−2544.
(45) Lamblin, M.; Nassar-Hardy, L.; Hierso, J.-C.; Fouquet, E.; Felpin, F.-X. *Adv. Synth. Catal.* **2010**, *352*, 33−79.